

Thermodynamic Consistency in Variable-Level Coarse Graining of Polymeric Liquids

A. J. Clark, J. McCarty, I. Y. Lyubimov, and M. G. Guenza*

Department of Chemistry and Institute of Theoretical Science, University of Oregon, Eugene, Oregon 97403, USA

(Received 16 May 2012; published 15 October 2012)

Numerically optimized reduced descriptions of macromolecular liquids often present thermodynamic inconsistency with atomistic level descriptions even if the total correlation function, i.e. the structure, appears to be in agreement. An analytical expression for the effective potential between a pair of coarse-grained units is derived starting from the first-principles Ornstein-Zernike equation, for a polymer liquid where each chain is represented as a collection of interpenetrating blobs, with a variable number of blobs, n_b , of size N_b . The potential is characterized by a long tail, slowly decaying with characteristic scaling exponent of $N_b^{1/4}$. This general result applies to any coarse-grained model of polymer melts with units larger than the persistence length, highlighting the importance of the long, repulsive, potential tail for the model to correctly predict both structural and thermodynamic properties of the macromolecular liquid.

DOI: [10.1103/PhysRevLett.109.168301](https://doi.org/10.1103/PhysRevLett.109.168301)

PACS numbers: 83.80.Sg, 83.10.Mj, 83.10.Rs

Relevant structural and dynamical properties of polymer liquids take place over a large range of length (and time) scales. The computational requirements often render it impractical or impossible to fully investigate such systems with atomistic level simulations. To overcome these limitations, many descriptions of polymeric liquids with reduced internal degrees of freedom, or coarse-grained (CG) descriptions, have been proposed. The tremendous interest that CG methods have generated is due to their capability of speeding up simulations, probing systems on larger length scales than conventional atomistic simulations [1–8].

The basis for any coarse grained description is the specification of effective interaction potential energies or forces between coarse grained units. Despite the growing interest in CG methods and their proven successes, most CG models are still limited in their potential application because of the empirical character of the effective interaction potentials upon which they rely. While a few CG approaches have been formally derived [9–12], most, for example the iterative Boltzmann inversion procedure where the meso-scale potential is optimized to reproduce the total correlation functions, and sometimes secondarily the pressure [4], rely on numerical optimization of their CG parameters through comparison with the related atomistic simulations or with experimental data. Unfortunately, numerically optimized CG potentials are in principle neither transferable to different systems, nor to the same system in different thermodynamic conditions, and they can not ensure consistency for properties different from the ones against which their parameters have been optimized [13]. This limits, dramatically, their generality and convenience.

In this Letter, we present an analytical formalism for the potential describing the interaction between CG units for a model of a polymer liquid where each molecule is represented as a chain of interpenetrating spheres with variable size and number, in variable thermodynamic conditions: we show that the CG model presented and the related

analytical potential ensure structural and thermodynamic consistency with the atomistic description. The model is general, as the potential is fully transferable and it is applicable to liquids of polymers with different molecular structure. The analytical form of the potential allows for the characterization of some general features of how thermodynamic properties and structure depend on the shape of the intermolecular potential between CG units.

In a polymeric liquid of monomer density, ρ_m , and number of polymers n , the size of the polymeric chain is defined by its radius-of-gyration, $R_g^2 = Nl^2/6$, with l the effective segment length between the center-of-mass (c.m.) of two monomers, and N the number of monomers in a chain. Here we are concerned about liquids of polyethylene (PE), for which $l = 0.437$ nm. Each polymer is represented as a chain of superimposing soft blobs, with N_b the number of monomers in one blob, $n_b = N/N_b$ the number of blobs in one chain, and blob size characterized by $R_{gb} = R_g/\sqrt{n_b}$. The correlation functions that describe the static structure of the blob CG model have been derived from the formal solution of a generalized Ornstein-Zernike (OZ) equation where monomeric sites are assumed to be real sites, and CG sites are assumed to be fictitious sites, in an extension of Krakoviack's *et al.* [14,15] original approach, and including the thread model polymer reference interaction site model (PRISM) monomeric description [16,17]. By assuming a Gaussian distribution of the monomers inside a blob and monomer interactions much shorter ranged than the size of the blob, which are reasonable approximations for subchains with N_b larger than the persistence length (for PE $N_b \geq 30$), an analytical blob-blob total correlation function, $\hat{h}^{bb}(r)$, was derived, and shown to be in quantitative agreement with the total correlation function from atomistic simulations [17].

Starting from $\hat{h}^{bb}(r)$ and given that the monomer direct correlation function, $c^{mm}(r)$, has a range shorter than the size of the CG unit, an analytical solution of the CG

potential is derived by approximating the Fourier transform of $c^{mm}(r)$ by its zero wave vector value, $c_0 = 4\pi \int_0^\infty r^2 c^{mm}(r)$. The effective direct correlation between blobs is given in Fourier space by

$$\hat{c}^{bb}(k) = -\frac{N_b \Gamma_b}{\rho_m} \frac{1 + n_b \Gamma_b \{ \hat{\Omega}^{mm}(k) - [\hat{\Omega}_{av}^{bm}(k)]^2 / \hat{\Omega}_{av}^{bb}(k) \}}{1 + n_b \Gamma_b \{ \hat{\Omega}^{mm}(k) - [\hat{\Omega}_{av}^{bm}(k)]^2 / \hat{\Omega}_{av}^{bb}(k) \}}, \quad (1)$$

where $\Gamma_b = -N_b \rho_m c_0$, $c_0 < 0$, and $\hat{\Omega}_{av}^{mm}(k)$, $\hat{\Omega}_{av}^{bm}(k)$, and $\hat{\Omega}_{av}^{bb}(k)$ are the chain-averaged intramolecular correlation functions between pairs of monomers, the c.m. of a blob and a monomer, and pairs of blob c.m.'s respectively, normalized so their value at $k=0$ is one. For wave vectors near $k=0$, the intramolecular correlations are approximately $\hat{\Omega}^{mm}(k) \approx 1 - n_b k^2 / 3 + n_b^2 k^4 / 12$, $\hat{\Omega}^{bm}(k) \approx 1 + (1/6 - n_b/3)k^2 + (3 - 5n_b - 10n_b^2 + 15n_b^3)k^4 / 180n_b$, and $\hat{\Omega}^{bb}(k) \approx 1 + (1/3 - n_b/3)k^2 + (2 - n_b - 4n_b^2 + 3n_b^3)k^4 / 36n_b$. The sharp peak around $k=0$ leads to the enhanced sensitivity of the function to the quality of the approximations used in the chain model, and made numerical solutions of the potential necessary in our previous work. The total correlation function in this blob description gives isothermal compressibility, $\kappa_T = [k_B T \rho_m (1 + \Gamma_b) / N]^{-1}$, with k_B the Boltzmann constant and T the temperature, which is consistent with the compressibility in the atomistic description [16]. Intra- and intermolecular pair distribution

functions and the structure factor are consistent with their atomistic counterpart for distances $r > R_{gb}$ and wave vectors $k < 2\pi / R_{gb}$.

Assuming that a coarse grained unit contains a number of monomers sufficiently large to follow a Gaussian space distribution, and that the density and the interaction strength are large enough that the product $\Gamma_b > 1$, the contribution to the inverse transform integral for large wave vectors ($k \gg 1/R_{gb}$) is negligible for $r > R_{gb}$. In this limit, the direct correlation for $k \ll 1/R_{gb}$ has the simple rational function limiting form $c^{bb}(k) \propto 1/(1 + \Gamma_b R_{gb}^4 k^4)$ as $\Gamma_b \rightarrow \infty$. Approximating the effective direct correlation by this form for all wave vectors introduces very little error, allowing for a simple approximation for the functional form in real space. The accuracy at intermediate Γ_b values can be improved by taking this as the zeroth order term of an asymptotic expansion in $1/\sqrt{\Gamma_b}$ about $\Gamma_b \rightarrow \infty$.

The effective potential is then derived by applying the approximation $V^{bb}(r) \approx -k_B T \{ c^{bb}(r) - h^{bb}(r) + \ln[1 + h^{bb}(r)] \} \approx -k_B T c^{bb}(r)$, the limiting form of the hypernetted chain approximation valid when $|h^{bb}(r)| \ll 1$ everywhere. This approximation holds for soft potentials in the limit of high densities and long chains of interest here [18]. For $r > R_{gb}$, the intermolecular blob potential, which is the needed input for the mesoscale simulations of the CG polymer liquid, is given by

$$V^{bb}(r) \approx k_B T \left\{ \left(\frac{45\sqrt{2}N_b \Gamma_b^{1/4}}{8\pi\sqrt{3}\sqrt[4]{5}\rho_m R_{gb}^3} \right) \frac{\sin(Qr)}{Qr} e^{-Qr} - \left(\frac{\sqrt{5}N_b}{672\pi\rho_m \Gamma_b^{1/4} R_{gb}^3} \right) \right. \\ \left. \times \left[(13Q_{rs}^3(Qr - 4)) \cos(Qr) + \left(\frac{945 + 13Q_{rs}^4}{\Gamma_b^{1/4}} \right) r \sin(Qr) + \frac{945r}{\Gamma_b^{1/4}} \cos(Qr) \right] \frac{e^{-Qr}}{Qr} \right\}, \quad (2)$$

where $Q = 5^{1/4} \sqrt{3/2} / (\Gamma_b)^{1/4}$, $Q_{rs} = 5^{1/4} \sqrt{3/2}$, and r is in units of the blob radius-of-gyration, R_{gb} . When $n_b = 1$, Eq. (2) represents the effective potential between the c.m. of two polymers in a melt.

Because the potential is formally expressed as a function of the molecular and thermodynamic parameters, Eq. (2) is in principle general and applicable to polymer melts in different thermodynamic conditions and with diverse macromolecular structures.

The range of the effective potentials between CG units scales beyond the effective blob radius of gyration, R_{gb} , and decays with the number of monomers per blob as $N_b^{1/4}$. The observed scaling behavior can be explained by considering that in a liquid the total effective correlation between two sites (atomistic or CG), and its related potential, can be regarded as ‘‘propagating’’ through sequences of direct pair interactions following the OZ integral equation theory. These many-body contributions to the pair interaction are not simply additive, and once mapped into the OZ pair

interaction, they result in a slowly decaying tail. Because of the Gaussian statistics that applies to the structure of long polymeric chains, the interaction between any intermolecular pair of blobs statistically propagates in the shared volume as a random walk following the random path of effective CG sites. In the relevant volume $V_b \propto R_{gb}^3 \propto N_b^{3/2} l^3$, the number of effective CG sites is of the order of $n'_b \propto \rho_m R_{gb}^3 / N_b \propto N_b^{1/2} \rho_m l^3$, leading to the observed scaling of $N_b^{1/4}$.

From the analytical form of the effective potential, Eq. (2), the pressure of the system can be calculated explicitly. Specifically in the high density, long chain limit, the pressure calculated in the virial route reduces to the simple expression

$$\frac{P}{\rho_c k_B T} \approx 1 - \frac{N c_0 \rho_m}{2}, \quad (3)$$

where $\rho_c = \rho_m / N$ is the chain density. Equation (3) is in agreement with the monomer level description [16], and does not depend on the level of coarse-graining of the

model selected. It should be noted that because both the pressure and the compressibility are consistent with monomer level PRISM, the equations of state predicted from the virial and compressibility routes will show the same small inconsistencies between the routes, which are inherent to the approximations in integral equation theory [16,18]. The important point is that the pressure and compressibility are left unchanged from the monomer level description by the coarse graining procedure on all levels.

To test the self consistency and the predictions of the effective potentials we performed molecular dynamics (MD) simulations of polymer melts using the LAMMPS simulation package [19], in parallel on the San Diego Supercomputer Center Trestles cluster accessed through the XSEDE project. Simulations were performed both at the atomistic level, by adopting the traditional united atom model (UA-MD) with the established set of UA potentials (intermolecular Lennard-Jones, harmonic bonds and angle potentials) [20–22] and at the CG mesoscale level (MS-MD) where each chain was represented as a collection of soft colloidal particles. MS-MD simulations for the $n_b = 1$ case have been described previously [23–25]. To extend the model to cases where $n_b > 1$, the effective bond between adjacent blobs was taken to be $V_{\text{bond}} = 3k_B T r^2 / (8R_{gb}^2) + V^{bb}(r) + k_B T \ln[1 + h^{bb}(r)]$, which enforces the correct distributions between adjacent blobs [17], and an angle potential between sequential triples on each chain which likewise enforces the correct angular probability distribution [26]. Blobs more than two apart on each chain were taken to interact via the intermolecular pair potential $V^{bb}(r)$ of Eq. (2). All mesoscale simulations used here are performed in the NVE (microcanonical) ensemble. Values of the c_0 parameter, entering Γ_b in Eq. (2) and the MS-MD, were taken from the UA simulations for short chains. For systems with large N , which were too slow to relax to be accessible through UA-MD, the c_0 parameter was extrapolated from the available UA data at small N at the same monomer density, using the form predicted from monomer level numerical PRISM theory, $c_0 = a + b/N$, with a and b optimized parameters. The values of c_0 obtained from this procedure were found to be generally consistent with calculations using long-established numerical monomer level PRISM models when an attractive part to the monomer potential is included [16].

Figure 1 displays the effective intermolecular force [$F^{bb}(r) = -\partial V^{bb}/\partial r$] between blobs, comparing the numerical solution of the potential with the approximate expression, Eq. (2). The approximate expression represents correctly the force in real space going from the peak to the long tail, which is the essential information needed for the correct calculation of thermodynamic properties. The inset in Fig. 1 shows the normalized Virial density [$N^{-2}r^3 F^{bb}(r)$], whose integral is proportional to the pressure, and which can be seen to be dominated by the tail region of the potential ($r > R_{gb}$). The peak of the force

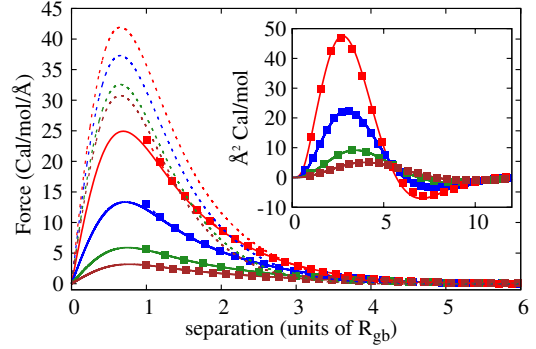


FIG. 1 (color online). Force curves for the $n_b = 1$ model (solid lines) and the approximated Eq. (2) (squares) for (top to bottom) $N = 100$ (red), $N = 200$ (blue), $N = 500$ (green), and $N = 1000$ (brown), along with force curves for models with a fixed blob length, $N_b = 50$, and increasing numbers of blobs (dashed lines, from top to bottom): $n_b = 2$ (red), $n_b = 4$ (blue), $n_b = 10$ (green), and $n_b = 20$ (brown). Inset: Normalized virial density [$N^{-2}r^3 F^{bb}(r)$] for the numerical forces (lines) and their analytical forms (squares) for $n_b = 1$. Degree of polymerization (N) increases from top to bottom at the peak below $5R_{gb}$. All systems are at 400 K and density $\rho_m = 0.03355 \text{ \AA}^{-3}$.

decreases with increasing blob length, N_b , at constant density, ρ_m , but its range increases in such a way that the Virial integral ultimately reaches a plateau, which corresponds to the leveling off of the pressure, as shown in Fig. 2. The inset of Fig. 1 also shows that the effective potential has a small attractive part at long range: such an attractive component is a necessary condition for a stable liquid to form, as a gas phase would be the state of lowest free energy at any temperature for a system of purely repulsive particles with no additional constraints. This attractive contribution is partially of entropic origin and

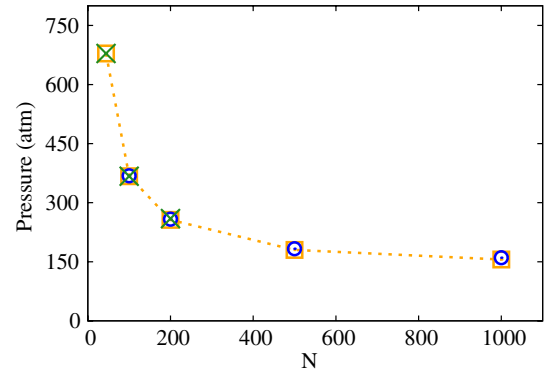


FIG. 2 (color online). Pressure measured from simulations with input CG forces from Fig. 1, where $n_b = 1$ (orange squares connected by dashed guide lines), and $N_b = 50$ with $n_b > 1$ (open blue circles). Also depicted are UA-MD simulations (green X symbols) for systems which relax fast enough for UA-MD to be feasible ($N \leq 200$). Data are collected for increasing degree of polymerization N , at the same values of N as Fig. 1. All simulations were performed at 400 K and density $\rho_m = 0.03355 \text{ \AA}^{-3}$.

partially due to the attractive component of the intermonomer potential. Figure 2 shows that all simulations of the same system, independent of the level of coarse graining, generate not only consistent structure, as seen before, but also consistent pressure.

The scaling of the potential is a property of the representation; increasing the number of monomers in each coarse grained unit on each chain, with a fixed system density and monomer interaction, results in an effective potential that grows long-ranged because it captures the average effect of the many-polymer correlations mapped into the effective pair interactions. This is a consequence of the fractal dimension of polymers, which is of order two, as blob volume increases with N_b faster than the chain can fill it, leading to an increasing with N_b of the level of chain interpenetration. If however, melts of increasingly long chains at the same density are represented by increasing numbers of soft blobs of fixed N_b , the range of the potential between blobs limits to a fixed value with increasing chain length as the direct correlation parameter c_0 approaches its limit.

Analysis of these results shows that the range of the effective potential is highly density dependent, both explicitly and indirectly through the direct correlation parameter, c_0 , as shown in Fig. 3. Also reported for comparison is the force generated from the potential of mean force, which is a very poor representation of the “real” force at high densities.

Finally, Fig. 4 compares predictions of pressure as a function of density for two samples with increasing chain length, i.e. $N = 44$ and $N = 100$. Data from MS-MD of the CG soft-blob representation show excellent agreement with data from UA-MD in the range where UA-MD were performed. The agreement appears to be independent of the level of CG representation that is adopted, as soft spheres and chains of soft blobs have

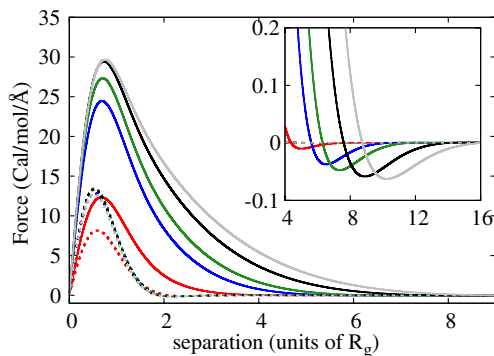


FIG. 3 (color online). Numerical force curves for $N = 100$, $n_b = 1$ models of PE with increasing densities (bottom to top) 0.03226 \AA^{-3} (red), 0.03355 \AA^{-3} (blue), 0.03441 \AA^{-3} (green), 0.03656 \AA^{-3} (black), and 0.03871 \AA^{-3} (gray), along with corresponding mean force curves (dashed lines, also from bottom to top). Inset: detail of the attractive contribution to the force (intercepts occur at increasing separation for increasing density). All systems are at 400 K.

consistent pressure across the different levels of coarse graining. The calculations are dominated by the presence of the long-ranged tail of the potential, further validating the proposed CG description. The range of separations over which the effective potential must represent the average of many-polymer effects increases dramatically with density. While all levels of representation accurately reflect whole-system thermodynamic averages and structural pair correlations, a coarse grained description may be unable to resolve processes below the length scale of the potential tail, due to this averaging effect.

The difference between the scaling predictions for the effective potential and the potential of mean force also has very important implications for theories of polymer melts. The strength of the potential of mean force, $w(r) = -k_B T \ln[1 + h^{bb}(r)]$, is found to scale for long chains, or large blobs, and high densities as $1/(\rho_m \sqrt{N})$ and its range as $N^{1/2}$ with c_0 becoming irrelevant and $w(r)$ vanishing in the infinite chain limit. Use of the $w(r)$ in thermodynamic relations therefore results in vanishing energies and pressures in the long chain or high density limit, which would imply the irrelevance of intermolecular interactions and allow reduction of the system to a single chain problem. While the effective pair potential at contact, $V^{bb}(0)$, still vanishes in the infinite chain limit, its tail increases in such a way that the Virial integral does not vanish. Likewise, the average effective energy in the system also does not vanish, and furthermore, both depend on the monomer level direct correlation, and therefore on the monomer interaction potential. This implies that even in the infinite chain limit, intermolecular potentials do not become irrelevant, and therefore cannot generally be neglected, as it is conventionally done in the description of polymer melt dynamics [27].

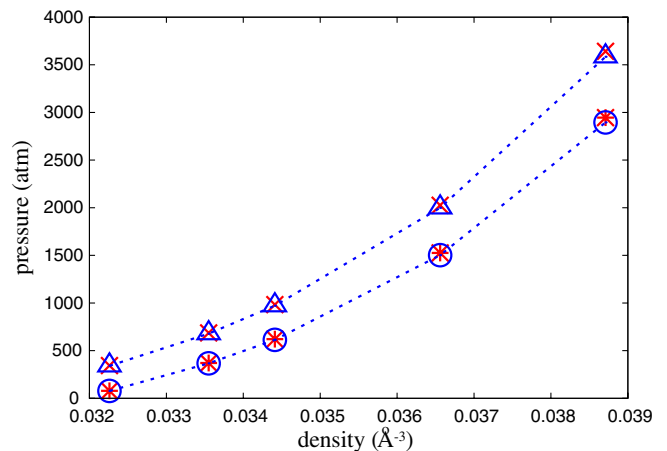


FIG. 4 (color online). Pressures measured in MS-MD simulations versus density, for $N = 44$ (triangles) and $N = 100$ (circles), performed with effective potentials where c_0 is determined from UA-MD simulations. Also reported are values from the corresponding UA-MD simulations (crosses for $N = 44$ and stars for $N = 100$). All simulations were performed at 400 K. Connecting lines are added as a guide to the eye.

In this Letter we have presented an analytical characterization of the soft pair potentials that arise in high level coarse grained descriptions of interpenetrating polymer melts, i.e., for soft-sphere and chains of soft-blob coarse graining mappings of polymer melts. The form of the potential and the pressure are obtained directly in terms of parameters from the monomer level theory, without a need for phenomenological correction forms in the potential and numerical optimization procedures. The effective potentials for these CG models show characteristic long-ranged “tails” that scale nontrivially with chain length, density, and monomer interaction strength. This family of CG models guarantees the consistency of the structure and thermodynamics of the macromolecular liquid in any level of soft representation, which is relevant in the modeling of complex polymeric liquids, as well as in the design of reliable multiscale modeling approaches to capture relevant phenomena that may occur on many different length scales. Dynamical properties will be accelerated in the CG representation, and will have to be properly rescaled to reconstruct the realistic dynamics [25].

We acknowledge support from the National Science Foundation through Grant No. DMR-0804145. Computational resources were provided by Trestles through the XSEDE project supported by NSF. This research was supported in part by the National Science Foundation under Grant No. PHY11-25915.

*Corresponding author.

mguenza@uoregon.edu

- [1] L. Jacobson and V. Molinero, *J. Phys. Chem. B* **114**, 7302 (2010).
- [2] J.J. de Pablo, *Annu. Rev. Phys. Chem.* **62**, 555 (2011).
- [3] A. Savelyev and G.A. Papoian, *Proc. Natl. Acad. Sci. U.S.A.* **107**, 20 340 (2010).
- [4] P. Carbone, H.A. Karimi, Varzaneh, X.Y. Chen, and F. Müller-Plathe, *J. Chem. Phys.* **128**, 064904 (2008).
- [5] V.A. Harmandaris, N.P. Adhikari, N.F.A. van der Vegt, and K. Kremer, *Macromolecules* **39**, 6708 (2006).
- [6] B.G. Levine, D.N. Le Bard, R. De Vane, W. Shinoda, A. Kohlmeyer, and M.L. Kein, *J. Chem. Theory Comput.* **7**, 4135 (2011).
- [7] T. Vettorel, G. Besold, and K. Kremer, *Soft Matter* **6**, 2282 (2010).
- [8] G. D’Adamo, A. Pelissetto, and C. Pierleoni, *Soft Matter* **8**, 5151 (2012).
- [9] S. Izvekov and G.A. Voth, *J. Phys. Chem. B* **109**, 2469 (2005).
- [10] J.F. Rudzinski and W.G. Noid, *J. Chem. Phys.* **135**, 214101 (2011).
- [11] P.G. Bolhuis, A.A. Louis, J.-P. Hansen, and E.J. Meijer, *J. Chem. Phys.* **114**, 4296 (2001).
- [12] G. Yatsenko, E.J. Sambriski, M.A. Nemirovskaya, and M. Guenza, *Phys. Rev. Lett.* **93**, 257803 (2004).
- [13] A.A. Louis, *J. Phys. Condens. Matter* **14**, 9187 (2002).
- [14] V. Krakoviack, J.-P. Hansen, and A.A. Louis, *Europhys. Lett.* **58**, 53 (2002).
- [15] V. Krakoviack, B. Rotenberg, J.-P. Hansen, *J. Phys. Chem. B* **108**, 6697 (2004).
- [16] K.S. Schweizer and J.G. Curro, *Chem. Phys.* **149**, 105 (1990).
- [17] A.J. Clark and M.G. Guenza, *J. Chem. Phys.* **132**, 044902 (2010).
- [18] J.-P. Hansen and I.R. McDonald, *Theory of Simple Liquids* (Academic, New York, 1990), 2nd ed.
- [19] S. Plimpton, *J. Comput. Phys.* **117**, 1 (1995).
- [20] M. Putz, J.G. Curro, and G.S. Grest, *J. Chem. Phys.* **114**, 2847 (2001).
- [21] M.G. Martin and J.I. Siepmann, *J. Phys. Chem. B* **102**, 2569 (1998).
- [22] E.K. Watkins and W.L. Jorgensen, *J. Phys. Chem. A* **105**, 4118 (2001).
- [23] J. McCarty, I.Y. Lyubimov, and M.G. Guenza, *J. Phys. Chem. B* **113**, 11 876 (2009).
- [24] J. McCarty, I.Y. Lyubimov, and M.G. Guenza, *Macromolecules* **43**, 3964 (2010).
- [25] I.Y. Lyubimov and M.G. Guenza, *Phys. Rev. E* **84**, 031801 (2011).
- [26] M. Laso, H.C. Ottinger, and U.W. Suter, *J. Chem. Phys.* **95**, 2178 (1991).
- [27] M. Doi and S.F. Edwards, *The Theory of Polymer Dynamics* (Oxford University, New York, 1986).